[5]Robinson, M. C. and Luttges, M. W., "Unsteady Flow Separation and Attachment Induced by Pitching Airfoils," AIAA Paper 83-0131, Jan. 1983.
[6]Harper, P. W. and Flanigan, R. E., "The Effect of Rate Change of Angle of Attack on the Maximum Lift of a Small Model," NACA TN-2061, 1950.
[7]Ham, N. D. and Garelick, M. S., "Dynamic Stall Considerations in Helicopter Rotors," *Journal of the American Helicopter Society*, July 1981, pp. 40-50.
[8]Francis, M. S., Keesee, J. E., and Retelle, J. P., "An Investigation of Airfoil Dynamic Stall with Large Amplitude Motion," U.S. Air Force Academy, Colorado Springs, CO., FJSRL-TR-83-0010, Oct. 1983.
[9]Deekens, A. C. and Kuebler, W. R., "A Smoke Tunnel Investigation of Dynamic Separation," *Aeronautics Digest*, USAF A-TR-79-1, Feb. 1979, pp. 2-16.
[10]Daley, D. C., "The Experimental Investigation of Dynamic Stall," Thesis, Air Force Institute of Technology, Wright-Patterson Air Force Base, OH, AFIT/GAE/AA/820-6, 1983.
[11]Walker, J. M., Helin, H. E., and Strickland, J. H., "An Experimental Investigation of an Airfoil Undergoing Large Amplitude Pitching Motions," *AIAA Journal*, Vol. 23, Aug. 1985, pp. 1141-1142.
[12]Jumper, E. J., "Theoretical Investigation of Dynamic Stall Using a Momentum Integral Method," *Proceedings from Workshop on Unsteady Separated Flow*, University of Colorado, Dept. of Aeronautical Engineering, Boulder, CO, Aug. 10-11, 1983, pp. 148-151.
[13]Jacobs, E. N. and Sherman, A., "Airfoil Section Characteristics as Affected by Variations of the Reynolds Number," NACA Rept. No. 586, *23rd Annual NACA Reports*, 1937, pp. 577-611.
[14]Gormont, R. E., "A Mathematical Model of Unsteady Aerodynamics and Radial Flow for Application to Helicopter Rotors," U.S. Army AMRDL Tech. Rept. 72-67, 1973.
[15]Liiva, J., Davenport, F. J., Gray, L., and Walton, I. C., "Two-Dimensional Tests of Airfoils Oscillating Near Stall," The Boeing Company, Vertol Div., U.S. Army Aviation Material Laboratories, For Eustis, VA, USAAVLABS Tech. Rept. 68-13, Vols. I and II, April 1968.
[16]Gray, L., Liiva, J., and Davenport F. J., "Wind Tunnel Tests of Thin Airfoils Oscillating Near Stall," The Boeing Company, Vertol Div., U.S. Army Aviation Material Laboratories, Fort Eustis, VA, USAAVLABS Tech. Rept. 68-89, Vols. I and II, Jan. 1969.

Simulation of Inviscid Vortex-Stretched Turbulent Shear-Layer Flow

Arthur Rizzi*
FFA The Aeronautical Research Institute of Sweden
Bromma, Sweden
and
Charles J. Purcell†
ETA Systems, Inc., St. Paul, Minnesota

Introduction

REALISTIC numerical simulations of vortex flows around aircraft require three-dimensional discrete models of significant size.[1] The recent construction of a 16-million-word memory for the CYBER 205 has allowed tests of 1-million-grid-point models on a practical basis within reasonable elapsed times. Prior to this it was hoped that this type of computation could be performed with disk I/O, but experience showed that heavy time penalties were encountered due to the demands of the flow-solving algorithm. Therefore, good virtual-memory-management techniques within a sufficient working set of *real* memory seem to be the only effective way to carry out such large-scale simulations. The other crucial requisite is a large bandwidth communciation channel between the memory and the arithmetic unit.

What do we expect to see in the inviscid simulation as the discrete model grows larger, with more and more grid points added in the discretization? For one thing, the accuracy will improve but, more importantly for the physical understanding, the allowable degrees of freedom in the solution increase so that we may begin to study fundamental flow instabilities such as the interacting of stretched vortices as described by the continuum equations. The advent of supercomputers with very large real memory just now offers the possibility to explore such phenomena numerically.

The type of vortex flowfield we want to simulate develops when a delta-shaped wing meets an oncoming stream of air at a high angle of attack. The flow separates from the wing in a shear layer along the entire sharp leading edge and, under the influence of its own vorticity, coils up to form a vortex over the upper surface of the wing. The high velocities in the vortex create a low-pressure region under it, which gives the wing a nonlinear lift. The flow also separates in a shear layer from the trailing edge of the wing, which forms into a wake vortex. The primary and wake vortices then interact with each other behind the wing. The appropriate model to describe the fluid mechanics of this vortex flow is the compressible Navier-Stokes equations. But if the Reynolds number of the flow is very large—say, over 10 million—the shear stresses and dissipation terms take effect only in very thin layers of the flow on the surface of the wing and across the shear layers that separate from the leading and trailing edges. For this type of flow, it is these free shear layers, and not the boundary layer, that contribute the greatest amount of vorticity. The intent of this paper is to study the dynamics and the stability of these free shear layers by means of numerical simulation. Because the layers are thin and not influenced by the no-slip boundary conditions, the shear stresses and dissipation terms do not have to be accurately represented. They can instead be modeled by simpler nonphysical expressions. In this way the equations we solve are the Euler equations with an artificial viscosity model. The flow, therefore, is inviscid except across thin discontinuities like shock waves and vortex sheets that are

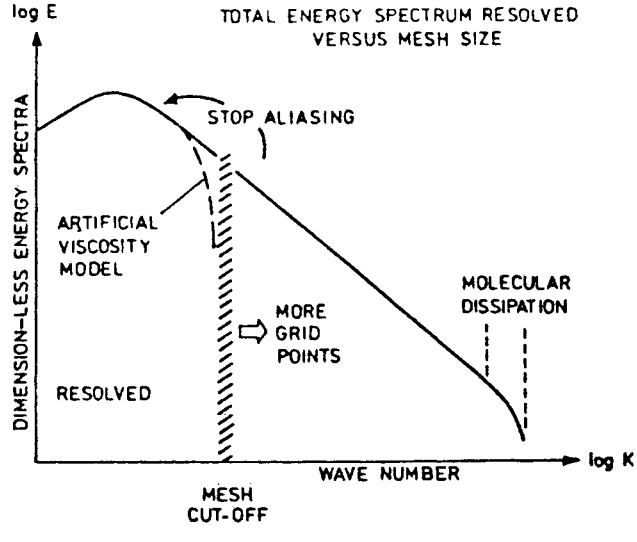

Fig. 1 Energy cascade of high Reynolds number turbulent flow.

Received March 20, 1985; revision received June 25, 1985.

*Research Scientist; also Adjunct Professor of Computational Fluid Dynamics, Royal Institute of Technology, Stockholm. Member AIAA.
†Principal Consultant.

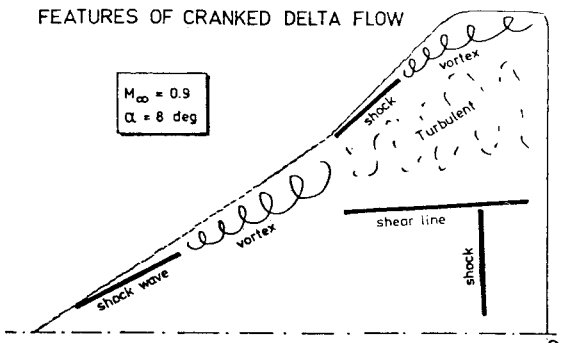

a) Schematic outline of main flow features.

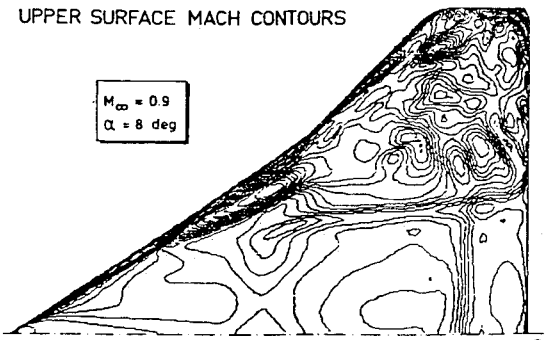

b) IsoMach contours.

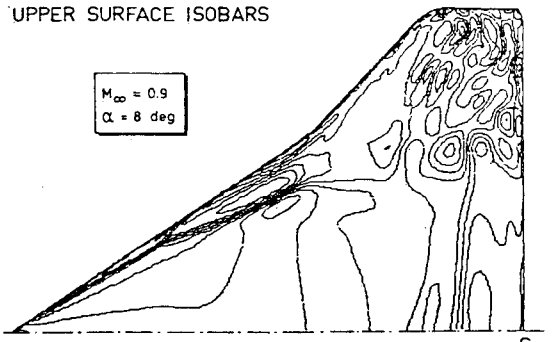

c) Isobars.

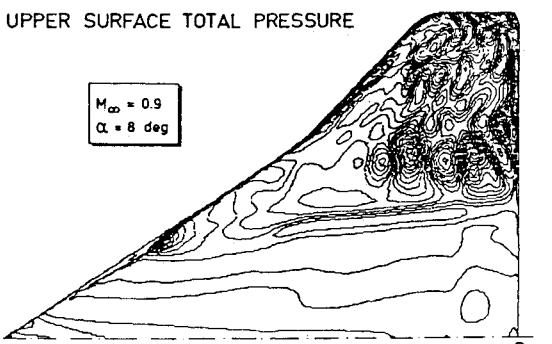

d) Total pressure contours.

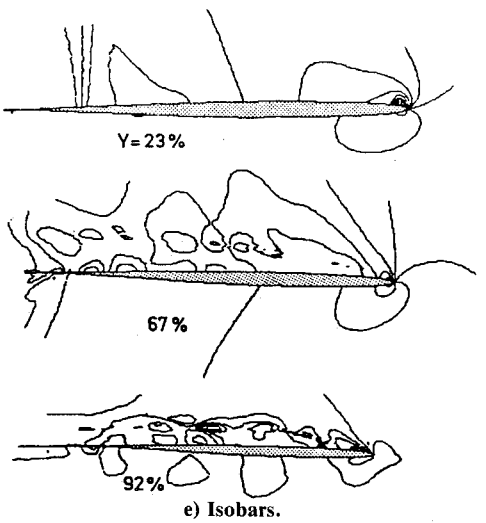

e) Isobars.

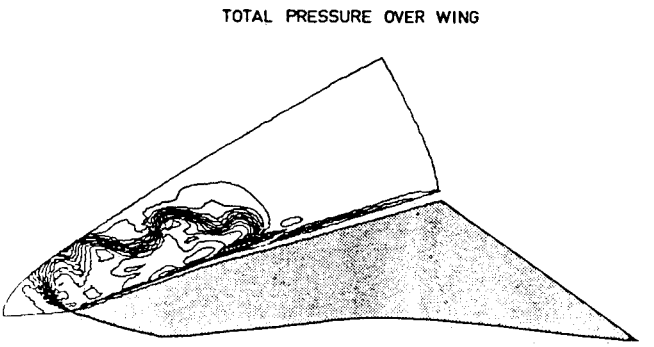

f) Total pressure contours.

Fig. 2 Inviscid compressible vortex flow highly stretched by a twisted cranked-and-cropped delta wing simulated by the Euler equations on a grid of 193 × 57 × 97 nodes.

admitted in the solution where irreversible processes can take place.

Discrete Flow Model

We use Eriksson's method of transfinite interpolation[2] to construct a boundary-conforming O-O-type mesh with just over 1 million cells around a cranked delta wing. The Euler equations can be expressed as an integral balance of the conservation laws

$$\frac{\partial}{\partial t}\iiint q\,d\nu + \iint H(q)\cdot n\,ds = \iint \Upsilon\cdot n\,ds \qquad (1)$$

where q is the vector with elements of mass, momentum, and energy. The flux quantity $H(q)\cdot n$ represents the net flux of q transported across, plus the pressure p acting on, the surface S surrounding the volume of fluid, and Υ is the artificial viscosity model. The finite volume method then discretizes 1) by assuming that q is a cell-averaged quantity located in the center of the cell and that the flux terms $H(q)\cdot n$ and $\Upsilon\cdot n$ are defined only at the cell faces by averaging the values on each side. A more detailed description of the method is given in Ref. 3. With the appropriate boundary conditions, a two-level, three-stage Runge-Kutta scheme steps the solution forward in time.

Vortex-Flow Simulation

The flow model we have described dissipates phenomena whose wavelength is on the order of the mesh spacing, and so it mimics the action of the real Newtonian viscosity, which for high Reynolds number flows acts on the molecular scale. Therefore, the smaller we make the mesh spacing by adding more grid points, the finer the scale length of the phenomena we can resolve without its being obliterated by the dissipation. We hypothesize that, given a sufficient number of grid points to support the small scales, the Euler equations do model the onset of turbulent flow with an inertial range in the energy spectrum (Fig. 1). The mechanism for the excitation, as well as

the probable instability of the small-scale flow features sustained by the transfer of energy from the large scales, is the stretching of vorticity caused by the external straining of the free shear layers and the shock waves in this transonic flow. This mechanism is expressed by the vorticity equation for compressible nonisentropic flow

$$\frac{D}{Dt}\frac{\omega}{\rho} = \frac{\omega}{\rho}\cdot E + \frac{1}{\rho^3}(\text{grad } \rho \times \text{grad } p)$$

where E is the rate-of-strain tensor.

The aim then is to test this hypothesis in a numerical experiment simulating a flow where the term $(\omega/\rho)\cdot E$ is large. This is feasible because the stretching and distorting of the primary vortex can be accentuated by the geometrical shape of the wing. Consider flow past a cropped delta whose leading edge is not a straight line nor does it even lie in a plane—a so-called cranked-and-cropped delta wing with twist. The core of the vortex generated by the leading edge inboard of the crank will not be straight, and its velocity field will strain the leading-edge vortex starting outboard of the crank. The simulated flow for $M_\infty = 0.9$ $\alpha = 8$ deg using a grid of $193 \times 57 \times 97$ nodes is displayed in Figs. 2. The first of these figures gives a schematic representation of the main discernible features in the isoMach lines on the upper surface of the wing. Inboard of the crank a leading-edge shock wave interacts with the primary vortex, while further aft the flow is rather smooth except for a shock and a shear line.

Outboard of the crank and shear line, it changes dramatically. The different leading-edge sweep causes the inboard vortex to degenerate from a well-ordered feature into many smaller-scale eddies with substantial transient frequencies. The mechanism for this physical flow instability is, we believe, the stretching of the vortex produced at the crank. Outboard of the crank, another shock and vortex appear along the leading edge. This vortex then runs into the side edge of the cropped tip, turns because of the shear flow separating from the edge, and degenerates into small eddies. The overall flow pattern suggests, qualitatively at least, the presence of large-scale coherent turbulence. This particular wing exists only as numbers in the computer; we have no measurements to compare with and therefore cannot yet assess the quantitative realism of the simulation. The integrated values of lift and drag, $C_L = 0.466$ and $C_D = 0.059$ are quite reasonable. Comparison of the flow simulated after 1000 time steps and 2000 time steps indicates that these values change very little and that the flow is at least statistically steady. The small eddies meander around the upper surface but not out of the flowfield. These first results seem to support the hypothesis of energy transfer to small scales by vortex stretching.

The turbulentlike character occurs not only on the wing surface but out in the field as well. The isobars in three chordwise surfaces (Fig. 2e) confirm the trend from laminar to turbulent flow. The highly compressible nature of this case is evident around the leading edge. It seems that the shock waves at the leading edge produce entropy layers that are shed into the field over the wing. This layer is reasonably thin, but Fig. 2f reveals its unstable wavelike character in the spanwise direction from the crank to the tip.

References

[1]Rizzi, A., "Modelling Vortex Flowfields by Supercomputers with Super-size Memory," *Aeronautical Journal,* April 1985, pp. 149-161.

[2]Eriksson, L.E., "Generation of Boundary-Conforming Grids Around Wing-Body Configurations Using Transfinite Interpolation," *AIAA Journal*, Vol. 20, Oct. 1982, pp. 1313-1320.

[3]Rizzi, A.W. and Eriksson, L.E., "Computation of Flow Around Wings Based on the Euler Equations," *Journal of Fluid Mechanics*, Vol. 148, Nov. 1984, pp. 45-71.

Application of Steady Shock Polars to Unsteady Shock Wave Reflections

G. Ben-Dor*
Ben-Gurion University of the Negev
Beer Sheva, Israel
and
K. Takayama†
Tohoku University, Sendai, Japan

IN the course of the present study, an experimental investigation of the dynamics of the MR→RR transition over concave cylinders was performed. It was found that the process goes through the following sequence of events: direct Mach reflection → stationary Mach reflection → inverse Mach reflection and finally transition to regular reflection. Furthermore, it is shown that the steady (P,θ) shock polars can be used in a special way to understand the transition process and also to explain the resulted wave configuration.

The present experimental study brings more light and understanding to this complex transition phenomenon over a concave cylinder. It is hoped that the present study will be of help to investigators interested in establishing the analytical transition criterion for this reflection phenomenon.

Present Study

Figure 1 illustrates the triple-point trajectory of the Mach reflection over the the concave cylinder. The experimental results indicate that the length of the Mach stem λ increases from $\lambda = 0$ to a maximum, after which it decreases until it vanishes ($\lambda = 0$) at the point where transition to regular reflection takes place. It should be noted that the first measured data point is not at the beginning of the cylindrical wedge; however, since λ must start from zero, a reasonable trajectory is drawn in dashed lines in the region where experimental data are unavailable. Consequently, the triple-point trajectory can be divided into two parts; a part in which $d\lambda/ds > 0$ and a part in which $d\lambda/ds < 0$, where s is a distance measured along the wedge surface.

Courant and Friedrichs[1] introduced three different types of Mach reflection depending upon whether the triple point moves away from, parallel to, or toward the reflecting wedge. These three different types of Mach reflection, which were termed by them direct Mach, stationary Mach, and inverse Mach reflections, are shown schematically in Fig. 2 as inserts A, B, and C, respectively.

Following Courant and Friedrichs,[1] one can conclude that the experimental measurement of the triple-point trajectory (Fig. 1) suggests that the reflection of a planar shock wave over a concave cylinder goes through the following sequence of events: a direct Mach reflection along the part where $d\lambda/ds > 0$, a stationary Mach reflection at the point where $d\lambda/ds = 0$, an inverse Mach reflection along the part where $d\lambda/ds < 0$, and finally a regular reflection after the point where the MR→RR transition occurs.

In order to get a better insight into this phenomenon, it was decided to divide the truly unsteady flow into a sequence of momentarily pseudosteady flows and to use the steady (P,θ) polars. Although the use of steady (P,θ) polars for truly

Received Feb. 28, 1984; revision received July 12, 1985.

*Associate Professor, Department of Mechanical Engineering.
†Associate Professor, Institute of High Speed Mechanics.